

ASA: Training-Free Representation Engineering for Tool-Calling Agents

Youjin Wang^{1*} Run Zhou^{1*} Rong Fu² Shuaishuai Cao³ Hongwei Zeng⁴ Jiaxuan Lu⁵
Sicheng Fan⁶ Jiaqiao Zhao⁷ Liangming Pan⁸

Abstract

Adapting LLM agents to domain-specific tool calling remains notably brittle under evolving interfaces. Prompt and schema engineering is easy to deploy but often fragile under distribution shift and strict parsers, while continual parameter-efficient fine-tuning improves reliability at the cost of training, maintenance, and potential forgetting. We identify a critical Lazy Agent failure mode where tool necessity is nearly perfectly decodable from mid-layer activations, yet the model remains conservative in entering tool mode, revealing a representation-behavior gap. We propose **Activation Steering Adapter (ASA)**, a training-free, inference-time controller that performs a single-shot mid-layer intervention and targets tool domains via a router-conditioned mixture of steering vectors with a probe-guided signed gate to amplify true intent while suppressing spurious triggers. On MTU-Bench with Qwen2.5-1.5B, ASA improves strict tool-use F1 from 0.18 to 0.50 while reducing the false positive rate from 0.15 to 0.05, using only about 20KB of portable assets and no weight updates.

1. Introduction

Large pretrained models demonstrate strong capabilities across a wide range of tasks, yet their efficient adaptation to specialized domains remains an open and practical challenge. In real-world deployments, the set of available tools, API signatures, and in-

teraction protocols changes frequently, and schemas continuously accumulate constraints, often leading to distribution shifts and breakdowns in output formats when a general model is applied to a concrete environment (Xi et al., 2025; Qin et al., 2023; Patil et al., 2024; Schick et al., 2023). The central engineering question is how to adapt a general model to evolving domain toolsets in a way that preserves its broad competencies while remaining stable and controllable in production (Hu et al., 2022; Dettmers et al., 2023; Prottasha et al., 2025). In this paper, we use *tool-calling domain adaptation* to denote robust *tool selection and tool-mode triggering* under *schema shift*, i.e., when available tools, API signatures, and interaction protocols evolve over time. This is especially difficult because tool calling is a discrete, parser-defined mode switch, so small distribution shifts can flip execution even when the underlying intent representation is preserved; moreover, the cost of updating prompts or adapters grows linearly with the number of domains and API versions, becoming prohibitive at scale.

Existing solutions follow two main directions. One direction operates on the input side by using prompts and schema constraints to steer tool invocation; this approach is easy to deploy but it consumes context capacity and is fragile under wording or context perturbations (Yao et al., 2022; Qin et al., 2023). The other direction adapts model parameters via parameter-efficient fine-tuning methods such as LoRA and its quantized variants; such methods improve in-domain invocation success and format compliance but impose recurring costs for training, deployment, and regression testing as domains and interfaces proliferate, and they risk degrading general capabilities over time (Hu et al., 2022; Dettmers et al., 2023; Tang et al., 2023; Prottasha et al., 2025; Lu et al., 2025).

When these approaches are deployed in dynamic or adversarial settings, three issues frequently arise. First, prompt and schema methods are brittle and sensitive to small changes in wording or context (Qin et al., 2023). Second, frequent fine-tuning is unsustainable

*Equal contribution ¹Renmin University of China
²University of Macau ³Central South University
⁴University of the Chinese Academy of Sciences ⁵Shanghai AI Laboratory ⁶Fudan University ⁷Central South University
⁸Peking University. Correspondence to: Liangming Pan <liangming.pan@pku.edu.cn>.

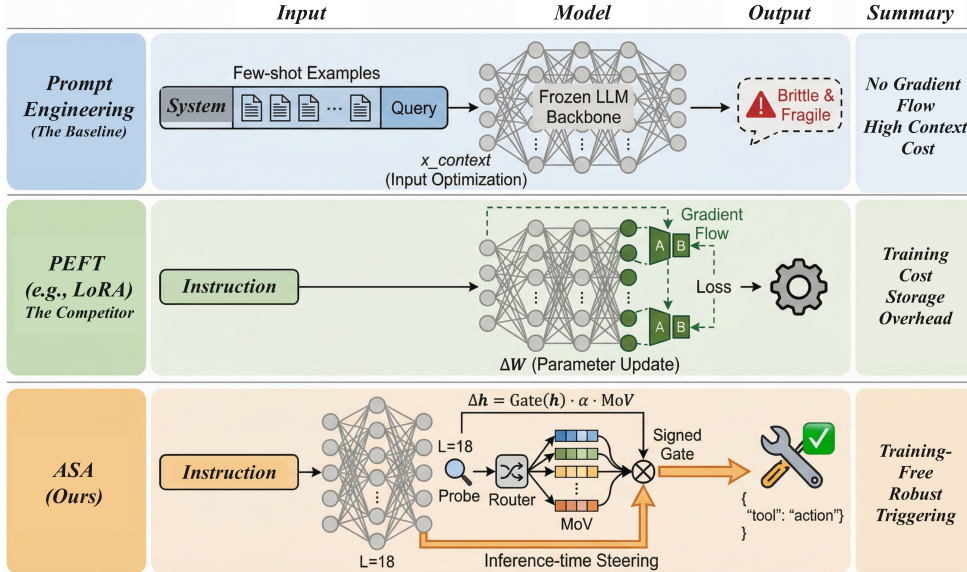


Figure 1. Overview of tool-calling domain adaptation methods under rapidly evolving tool sets and interaction protocols, and our inference-time probe-gated activation control.

at scale because the operational burden and risk of forgetting increase with the number of domains and interface versions (Hu et al., 2022; Dettmers et al., 2023; Prottasha et al., 2025). Third, there is a conceptual mismatch in treating tool invocation as mere knowledge or format injection rather than as a control problem that requires a reliable switch in the model’s execution mode. Empirically, we uncover a paradox that we term ‘Lazy Agent failure mode’: linear probes on mid-layer activations can predict tool necessity with near-perfect accuracy ($> 99\%$ AUC), yet the model’s overt generation fails to trigger tools in over 80 percent of these cases. This reveals a persistent *representation-behavior gap*, characterizing a state where the agent ‘knows’ what to do but lacks the activation impulse to break the generation threshold. Meanwhile, naive activation injection can also amplify spurious triggers due to downstream nonlinearities and adversarial constraints. This reveals a key bottleneck at the behavior-control layer (Zou et al., 2023; Turner et al., 2024; Wehner et al., 2025; Bartoszcz et al., 2025). This Lazy Agent failure mode characterizes a specific breakdown where tool-use intent is cleanly encoded within the representation space, but fails to cross the discrete decision threshold required for execution. Such a gap renders the model’s tool-calling capabilities brittle, as the latent “intent” and final “action” are effectively decoupled under strict parsing constraints. To resolve this, we argue that the agent requires more than just static guidance; it needs an inference-time control layer capable of bridging the representation-behavior gap.

Motivated by these observations, we propose a two-level, inference-time control paradigm that requires no weight updates. The approach models domain adaptation for agent-style tool-calling as a combination of representation-level intent alignment and decision-level boundary calibration (Zou et al., 2023; Turner et al., 2024; Wehner et al., 2025). At the representation level we introduce ASA, a compact adapter that models intent geometry using a shared base vector plus a small set of domain offset experts combined by a lightweight router. At the decision level, instead of logit-level biasing, we use a *probe-guided signed gate* that conditionally *opens* (injects) or *inverts* (suppresses) the steering direction, thereby calibrating the discrete tool-mode transition under strict tool-call parsing and adversarial phrasing (Lee et al., 2024; Rahn et al., 2024). On the MTU-Bench benchmark, ASA provides strong intent-aligned control with negligible storage and no training, yielding consistent improvements in strict F1 (balancing missed calls and false triggers) while largely preserving output format and argument compliance. Together, these findings suggest a practical middle ground that is more robust than prompt-only approaches and considerably lighter-weight than continual fine-tuning.

This positions tool calling as a form of *complex structural behavior control*, which is precisely where existing RepE-style steering is under-explored and where ASA is designed to operate. Our main contributions are threefold. First, we identify a *representation-behavior gap* in tool-calling adaptation: tool intent is

nearly perfectly linearly decodable from mid-layer activations, yet strict tool-mode triggering remains conservative, causing missed calls and false triggers. Second, we propose ASA, a training-free, inference-time activation controller that performs a *single-shot* mid-layer intervention using a router-conditioned *mixture-of-vectors* and a probe-guided *signed gate*; the gate acts as a context-aware safety valve, enabling bidirectional control with one strength knob α and optimizing strict F1 (Recall–FPR). Third, we introduce a strictly isolated MTU-Bench protocol with deterministic triggering and post-trigger validity checks (format/tool/args), and show consistent strict-F1 gains across prompt baselines, LoRA references, and model scales (0.5B/1.5B/8B), with only KB-level portable assets, under strict production constraints.

2. Related Work

2.1. LLM agents and tool-calling

LLM agent and tool-calling research integrates external tools into the reasoning/decision loop so models can query, compute, and interact with environments. Most approaches operate at the I/O interface through structured prompting, exemplars/templates, or output normalization and work well in relatively controlled settings. ReAct interleaves reasoning and actions but is prompt-fragile under wording or context shifts (Yao et al., 2022). Reflexion uses self-reflective memory but relies on stable traces and protocol assumptions (Shinn et al., 2023). Skill-accumulating agents such as Voyager compose procedures yet often bind to a specific interface, limiting cross-domain/protocol transfer (Wang et al., 2023). Output-side supervision or normalization (e.g., Toolformer and parsability-focused methods) improves reliability, but typically requires re-training or strong constraints when schemas evolve or prompts become adversarial (Schick et al., 2023; Johnson et al., 2025; Dang et al., 2025). Overall, prior work strengthens external workflows but offers limited mechanisms for internally stable, transferable execution-mode switching; we instead study internal control via mid-layer intent routing with lightweight gated calibration to robustly trigger tools without weight updates.

2.2. Parameter-efficient fine-tuning and domain adaptation

Parameter-efficient fine-tuning (PEFT) adapts pre-trained models to new domains with minimal additional parameters and computation. Representative PEFT variants include prompt-based methods such as Prefix-Tuning (Li & Liang, 2021), sparse parameter

updates like BitFit (Zaken et al., 2022), and low-rank adaptation approaches such as LoRA and QLoRA, which use low-rank updates to reduce fine-tuning costs (Hu et al., 2022; Dettmers et al., 2023). Tool-use datasets such as ToolAlpaca further show that PEFT can increase in-domain invocation success and format compliance (Tang et al., 2023). However, PEFT is training-driven: as domains and interfaces proliferate and change, training, deployment, regression testing, and rollouts scale roughly linearly, with risks of forgetting and version drift. ReFT constrains updates to low-dimensional subspaces to improve stability, but still requires training and thus struggles under rapid protocol churn (Wu et al., 2024). Other approaches (e.g., SK-Tuning) assume stable semantic anchors, which may not hold when alignment targets evolving function-call schemas (Prottasha et al., 2024). In contrast, we perform inference-time domain alignment via a switchable two-level control mechanism that leaves base weights untouched, reducing long-term maintenance burden.

2.3. Representation engineering and activation steering

Representation engineering and activation steering guide behavior by intervening on intermediate activations, enabling switchable and often interpretable control without retraining. Prior work shows that concepts/intentions can be detected and injected along activation directions to steer outputs (Zou et al., 2023; Turner et al., 2024). Yet most studies focus on single concepts or narrow tasks, and rarely model multi-domain geometry with shared bases plus domain-specific offsets. Further, representation-level interventions may not translate to end-to-end behavioral change under strong constraints or adversarial prompts, since downstream nonlinearities can attenuate injected signals. Taxonomies and systematization efforts improve selectivity and interpretability (Wehner et al., 2025; Bartoszcz et al., 2025), while conditional control methods refine intervention precision (Lee et al., 2024; Rahn et al., 2024). Most RepE work targets semantic attributes, whereas agent tool calling is a parser-defined *discrete mode switch* with strict executability constraints. Evidence on RepE for such multi-tool, schema-constrained *tool-mode switching* is limited; ASA addresses this by domain-structured directions with confidence gating.

3. Methodology

This section presents ASA, an inference-time mechanism designed to control whether a pre-trained language model enters a tool-invocation execution mode.

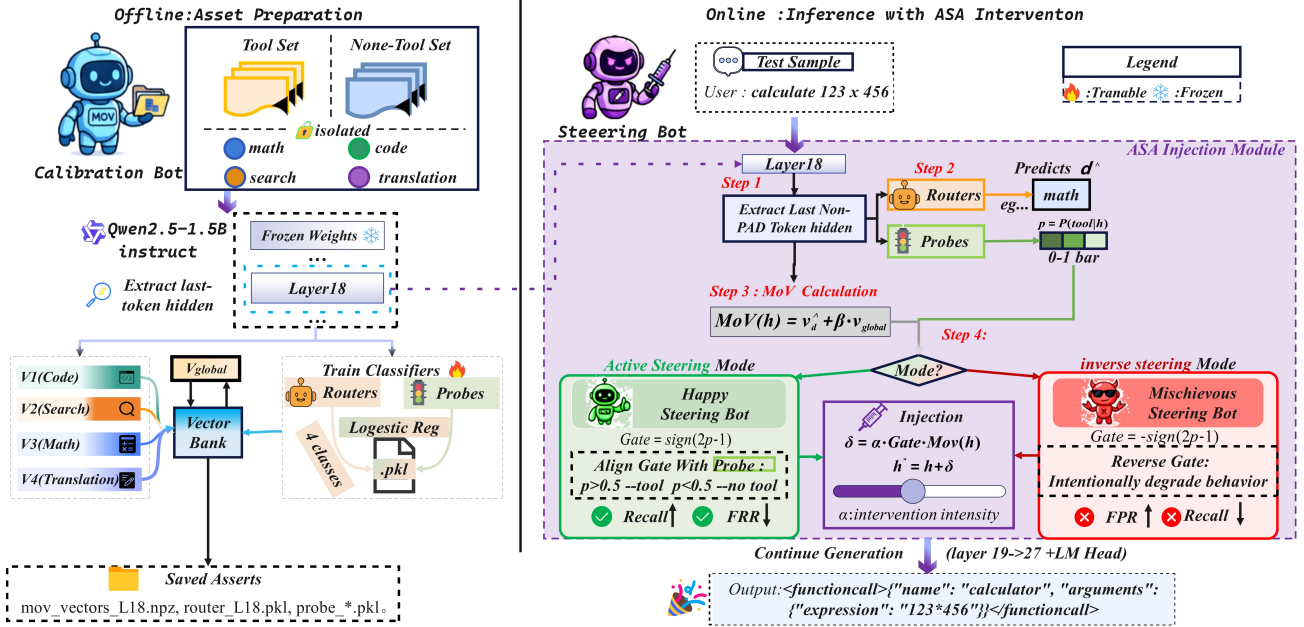


Figure 2. ASA overview. We extract the last-token hidden state at layer L during the pre-fill pass, route the input to a domain \hat{d} , estimate tool intent probability p , construct $\text{MoV} = v_{\hat{d}} + \beta v_{\text{global}}$, and inject $\Delta h = \text{Gate}(h) \cdot \alpha \cdot \text{MoV}$ once. No further interventions are applied during incremental decoding.

Table 1. H1 results at $L18$: tool intent is nearly perfectly linearly readable.

Model	Layer	AUC (Tool-Necessary vs. Non-Tool)	Shuffle AUC
Qwen2.5-0.5B-Instruct	18	0.9994	0.4982 [0.4891, 0.5076]
Qwen2.5-1.5B-Instruct	18	0.9996 [0.9987, 1.0000]	0.4966 [0.4884, 0.5053]
Qwen2.5-8B-Instruct	18	0.9989	0.4975 [0.4879, 0.5068]

Table 2. H3 results: cross-domain interference matrix (normalized diagonal).

	CODE	MATH	SEARCH	TRANSLATION
CODE	1.00	0.17	0.37	0.42
MATH	0.17	1.00	0.29	0.11
SEARCH	0.37	0.29	1.00	0.03
TRANSLATION	0.42	0.11	0.03	1.00

ASA is motivated by diagnostic observations about how tool-use intent is represented and causally expressed in intermediate activations. The method achieves reversible, low-cost control via a single hidden-state perturbation applied at a selected intermediate layer, while leaving backbone parameters unchanged.

3.1. Problem definition

We consider an autoregressive model that maps an instruction x to an output token sequence $y = (y_1, \dots, y_T)$. At generation step t , the model produces logits

$$z_t(x, y_{<t}) \in \mathbb{R}^{|V|}, \quad (1)$$

Table 3. H2 results (Qwen2.5-1.5B-Instruct, $L18$): injecting the intent direction changes tool-trigger evidence.

α	Direction	ΔLogit (mean)	ΔProb (mean)	p -value ($+v/-v$ vs. rand)
0.25	$+v$	+0.2077	+1.38%	2.51×10^{-36}
0.25	$-v$	-0.2230	-1.41%	1.89×10^{-37}
0.25	random	-0.0037	+0.11%	—
1.00	$+v$	+0.8359	+5.47%	7.10×10^{-43}
1.00	$-v$	-0.9414	-5.46%	3.26×10^{-44}
1.00	random	-0.0459	-0.22%	—

where V denotes the vocabulary, and corresponding probabilities $p_t = \text{softmax}(z_t)$. Here and below a deterministic parser defines a binary behavioral event

$$T(x) \in \{0, 1\}, \quad (2)$$

where $T(x) = 1$ if and only if the generated sequence is interpreted as a valid tool invocation by the parser (for example by containing a function-call scaffold whose syntax and arguments are parseable). The operational objective is to design a compact, portable controller that, for any input x , can increase the probability of producing a correct tool call when a tool is necessary while suppressing spurious calls when it is not, without modifying the model parameters θ .

3.2. Notation and measurement primitives

Extract the Pre-LN residual-stream representation at a chosen layer L and at the final non-padding prompt

token:

$$h_L(x) \in \mathbb{R}^D, \quad (3)$$

where D is the residual dimension. In experiments we also standardize each coordinate of h_L using training-set statistics; formally,

$$\tilde{h}_L(x) = \text{Std}(h_L(x)) = \frac{h_L(x) - \mu_{\text{train}}}{\sigma_{\text{train}}}, \quad (4)$$

where μ_{train} and σ_{train} denote per-dimension mean and standard deviation computed on the router/probe training partition.

For evaluation of causal influence we measure the mean change in logits for a set of trigger tokens \mathcal{S} . Given an intervention that maps $h_L \mapsto h'_L$, define

$$\Delta \text{Logit} = \mathbb{E}_{t \in \mathcal{S}} [z_t^{\text{trigger}}(h'_L) - z_t^{\text{trigger}}(h_L)], \quad (5)$$

where z_t^{trigger} denotes the logit(s) associated with tokens considered evidence of tool invocation and the expectation averages over the trigger positions.

3.3. Empirical diagnostics (motivation summary)

Three empirical findings justify the ASA design. First, a lightweight linear classifier trained on $h_L(x)$ reliably separates samples requiring tool invocation from those that do not, demonstrating that tool intent is linearly readable in mid-layer activations. Second, a direction derived from class-conditional means produces a measurable causal effect on early tool-trigger logits (Eq. (5)), far surpassing norm-matched random perturbations. Third, when intent directions are estimated separately per domain, the resulting vectors display partial domain-specific geometry, which implies that routing to domain-aware directions can reduce cross-domain interference.

3.4. ASA architecture and operations

ASA composes three lightweight components: a compact set of steering vectors, a multi-class router, and per-domain intent probes. At inference time ASA performs a single-shot, signed injection into $h_L(x)$ followed by normal forward propagation. Below we formalize each component and the intervention rule.

3.4.1. STEERING VECTOR CONSTRUCTION

Using a disjoint calibration split, compute class-conditional means in the layer- L hidden space:

$$\mu_{\text{pos}} = \mathbb{E}[h_L(x) \mid y^*(x) = 1], \quad (6)$$

$$\mu_{\text{neg}} = \mathbb{E}[h_L(x) \mid y^*(x) = 0], \quad (7)$$

where $y^*(x)$ is an oracle binary label indicating whether a tool call is necessary. The global intent vector is defined as

$$v_{\text{global}} = \mu_{\text{pos}} - \mu_{\text{neg}}, \quad (8)$$

where $v_{\text{global}} \in \mathbb{R}^D$ points from the non-tool mean toward the tool-necessary mean. Per-domain vectors v_d are built analogously by restricting expectations to samples in domain d . After construction, normalize each vector:

$$\hat{v} = \frac{v}{\|v\|}, \quad (9)$$

where $\|\cdot\|$ denotes the Euclidean norm and \hat{v} denotes the unit-normalized direction used at inference.

3.4.2. ROUTER AND PROBE DEFINITIONS

A lightweight router maps standardized representations to a domain label. Concretely,

$$\hat{d} = \arg \max_{d \in \mathcal{D}_{\text{dom}}} \text{softmax}(W^r \tilde{h}_L(x) + b^r)_d, \quad (10)$$

where $W^r \in \mathbb{R}^{|\mathcal{D}| \times D}$ and b^r are router parameters estimated on the router training split.

Each domain has a linear probe that outputs an intent score. For domain \hat{d} ,

$$p(x) = q_{\psi}^{(\hat{d})}(h_L(x)) = \sigma(w_{\hat{d}}^{\top} h_L(x) + b_{\hat{d}}), \quad (11)$$

where $\sigma(\cdot)$ is the sigmoid function, and $w_{\hat{d}}, b_{\hat{d}}$ are fitted on domain-specific training data. Here $p(x)$ estimates the probability that a tool invocation is appropriate.

3.4.3. MIXTURE-OF-VECTORS (MoV) COMPOSITION

Given the router prediction \hat{d} and the normalized vectors, ASA composes a direction using a domain expert plus a global offset:

$$\text{MoV}(h_L(x)) = \hat{v}_{\hat{d}} + \beta \hat{v}_{\text{global}}, \quad (12)$$

where $\beta \geq 0$ controls the strength of the global intent contribution and both $\hat{v}_{\hat{d}}$ and \hat{v}_{global} are unit-normalized as in Eq. (9). This modular design lets ASA scale to new domains by simply adding a new expert vector v_{new} (and updating the router), without retraining the backbone, effectively enabling a plug-and-play library of domain skills.

3.4.4. CONFIDENCE GATING AND SIGNED INJECTION

To avoid ambiguous injections near decision boundaries, map the probe probability to a ternary control

signal:

$$\text{Gate}(h_L(x)) = \begin{cases} +1, & p(x) > \tau, \\ -1, & p(x) < 1 - \tau, \\ 0, & \text{otherwise,} \end{cases} \quad (13)$$

where $\tau \in (0.5, 1)$ is a fixed confidence threshold selected on validation data.

The single-shot intervention applied at layer L is

$$h'_L(x) = h_L(x) + \text{Gate}(h_L(x)) \cdot \alpha \cdot \text{MoV}(h_L(x)), \quad (14)$$

where $\alpha \geq 0$ scales the perturbation magnitude. When probe is confident that a tool is required the controller adds the composed steering vector; when the probe is confident that no tool is needed the controller subtracts the vector; otherwise no modification is made. The injection occurs only once during the pre-fill pass and is not repeated at subsequent decoding steps.

3.5. Data hygiene and deployment constraints

To prevent leakage between calibration and evaluation, ASA uses disjoint data partitions. The calibration corpus is reserved solely for steering-vector estimation and is never used to train routers or probes. Router and probe fitting, hyperparameter selection including τ and α , and final reporting are performed on separate training/validation/test splits drawn from the benchmark partition. Standardization statistics in Eq. (4) are computed on the router/probe training split and applied at inference time.

The ASA asset footprint consists only of the small set of unit vectors $\{\hat{v}_d\} \cup \{\hat{v}_{\text{global}}\}$ and linear predictors $W^r, b^r, \{w_d, b_d\}$, making the controller portable and inexpensive to store and transmit.

3.6. Causal check and evaluation diagnostics

As a validation of causal efficacy, one computes the change in trigger logits under sign-symmetric injections and compares this to random-direction controls using Eq. (5). Sign-consistent ΔLogit values confirm that the constructed directions influence early trigger evidence. Behavior-level metrics such as strict trigger recall, false positive rate, and post-trigger executability are reported under a deterministic decoding protocol to minimize stochastic variability.

3.7. Inference summary

At runtime the controller is executed as a single, lightweight forward hook at layer L . The hook standardizes the last-token residual $h_L(x)$, predicts a do-

Algorithm 1 ASA single-shot inference (equation-referenced)

Require: Frozen model f_θ , router parameters (W^r, b^r) , per-domain probes $\{w_d, b_d\}$, steering vectors $\{\hat{v}_{\text{global}}, \hat{v}_d\}$, intervention layer L , strength α , global weight β , confidence threshold τ

- 1: Run the initial pre-fill forward pass and extract the last-token hidden state $h_L(x)$ from the Pre-LN residual stream.
- 2: Standardize the representation: compute $\tilde{h}_L(x) = \text{Std}(h_L(x))$ as in Eq. (4).
- 3: Predict domain label \hat{d} using the router: $\hat{d} \leftarrow \arg \max_d \text{softmax}(W^r \tilde{h}_L(x) + b^r)_d$. See Eq. (10).
- 4: Compute intent probability $p(x)$ from the domain probe: $p(x) \leftarrow \sigma(w_d^\top \tilde{h}_L(x) + b_d)$. See Eq. (11).
- 5: Form the routed steering direction $\text{MoV}(h_L(x)) \leftarrow \hat{v}_{\hat{d}} + \beta \hat{v}_{\text{global}}$ as in Eq. (12).
- 6: Evaluate the ternary gate $\text{Gate}(h_L(x))$ according to Eq. (13) using threshold τ .
- 7: Apply the single-shot signed injection:

$$h'_L(x) \leftarrow h_L(x) + \text{Gate}(h_L(x)) \cdot \alpha \cdot \text{MoV}(h_L(x)),$$

which implements Eq. (14).

- 8: Continue the forward pass from layer L using $h'_L(x)$ and decode autoregressively (no further injections).
- 9: **return** generated sequence y .

main, evaluates intent via the appropriate probe, composes the steering direction using Eq. (12), computes the ternary gate in Eq. (13), applies the signed injection in Eq. (14) if warranted, and then resumes the normal forward computation. The process leaves the base model parameters untouched and restricts interventions to a single temporal point.

4. Experiments

In this section, we evaluate ASA for tool-calling domain adaptation, focusing on its effectiveness under a strict experimental protocol, its controllability enabled by context-aware probe-guided gating, and its robustness across different model scales. We benchmark against prompt-only variants and a parameter-update baseline (LoRA) to clarify where ASA sits on the robustness–efficiency spectrum. All experiments are conducted on strictly isolated calibration, training, validation, and held-out test splits to prevent data leakage and to directly measure whether steering can bridge the representation and behavior gap. Additional visualizations are provided in Appendix E.

Table 4. LLaMA (8B, L=23) neighborhood adaptation (main results). We report triggering Precision/Recall/F1, Accuracy, and FPR for each domain. **ASA (Ours)** reports the best operating point per domain by F1 (from the α sweep).

Method	Metric	Code	Math	Search	Translation	ALL
Prompt-only	Precision (P)	0.8723	0.6857	0.8584	0.9382	0.8627
	Recall (R)	0.2854	0.3528	0.2629	0.9989	0.4988
	F1-Score	0.4218	0.4639	0.3957	0.9687	0.6238
	Accuracy (Acc.)	0.6358	0.6189	0.6287	0.9658	0.7159
	FPR	0.0389	0.1428	0.0367	0.0859	0.0829
Baseline	Precision (P)	0.8574	0.6368	0.8337	0.9234	0.8407
	Recall (R)	0.2508	0.2919	0.2089	0.9988	0.4378
	F1-Score	0.3879	0.4008	0.3339	0.9608	0.5759
	Accuracy (Acc.)	0.6049	0.5629	0.5839	0.9589	0.6779
	FPR	0.0419	0.1669	0.0419	0.0839	0.0839
ASA (Ours)	Precision (P)	0.9091	0.9987	0.9167	0.9241	0.9079
	Recall (R)	0.4167	0.9569	0.4583	0.9991	0.7188
	F1-Score	0.5714	0.9772	0.6111	0.9612	0.8023
	Accuracy (Acc.)	0.6875	0.9783	0.7083	0.9587	0.8229
	FPR	0.0370	0.0013	0.0350	0.0828	0.0700

4.1. Experimental Setup and Metrics

Benchmark construction. We evaluate on a 1,600-sample multi-domain benchmark spanning MATH, CODE, SEARCH, and TRANSLATION. Samples are constructed from public instruction-following and QA datasets (e.g., Alpaca (Stanford, 2023) and Natural Questions (Kwiatkowski et al., 2019)). We apply domain-specific filtering rules to form Tool-Necessary and Non-Tool pairs, validate tool labels via explicit $\langle\text{functioncall}\rangle$ markers, and randomly subsample 1,600 instances for evaluation (an engineering choice; the construction procedure scales to larger corpora). Detailed training and inference configurations of the LoRA baseline are provided in Appendix C.4.

Strict protocol and metrics. We count a tool call as *triggered* iff the output contains $\langle\text{functioncall}\rangle$. We report triggering Precision/Recall/F1, Accuracy, and FPR (Non-Tool trigger rate), plus Success Precision P_{succ} conditioned on triggering: JSON-valid (AST fallback), schema-consistent (whitelist), and argument-valid (present, non-empty, format-compliant). We select L by a probe sweep (best val AUC; Fig. 3), tune α by best val F1 (test sweep in Table 5), and tune τ on val (grid $\{0.50, 0.55, 0.60, 0.65, 0.70\}$) then fix it on test. Routers/probes use only train; vectors use only CAL.

4.2. Main Results on Two Models

We report results on two instruction-tuned LLMs: LLaMA (8B) and Qwen2.5-1.5B. Table 4 summarizes

domain-wise triggering performance on LLaMA. For each domain, ASA reports the best operating point selected by F1 from the α sweep, and we specially highlight our results. Table 5 further reports a full α sweep on Qwen2.5-1.5B under the same strict protocol, together with prompt variants and PEFT baselines, to situate ASA on the robustness–efficiency spectrum. ASA consistently improves the trigger-quality trade-off over both Prompt-only and Baseline across the two evaluated models (Tables 4, 5). On LLaMA, gains concentrate on domains that are not already saturated, while false triggers remain controlled; TRANSLATION is near ceiling on this split and thus exhibits limited headroom. On Qwen2.5-1.5B, prompt-only baselines either under-trigger (e.g., the system-free setting collapses tool calling) or trade higher recall for substantially more false alarms, underscoring the brittleness of prompt engineering under strict interfaces. In contrast, ASA improves triggering behavior across a broad range of steering strengths without inducing structural collapse: post-trigger validity remains stable, indicating that activation injection primarily modulates the decision to enter tool mode rather than corrupting formatting or argument construction. This is enabled by **probe-guided dynamic gating**, which conditionally opens or suppresses steering based on the current context, allowing ASA to mitigate the typical recall–hallucination trade-off.

Comparison across adaptation paradigms. Under the same strict protocol (Table 5), prompting mainly shifts surface instructions and tends to move along a recall–false-trigger frontier without reliably

Table 5. Results on the MTU-Bench test set (Qwen2.5-1.5B, $L=18$). ASA (Ours) applies probe-guided dynamic gating for all α ; we report **F1** as primary metric. Here *Trig. Prec.* denotes precision of the tool-mode triggering decision, while post-trigger validity (Format/Exec. Prec./Args) measures executability conditional on triggering, where **Exec. Prec.** is defined as the ratio of samples with both valid format and tool name to the total triggered samples.

α	Method	Branch	Triggering					Post-trigger validity			Cost		Rel. vs. baseline				
			Trig.	Prec.	Rec.	F1	Acc.	FPR	Format	Exec.	Prec.	Args	Storage	Train	$\Delta F1$	Δ Prec	Δ FPR
Prompt variants																	
Prompt: no_system			0.0000	0.0000	0.0000	—	0.0000	—	—	—	—	—	0	No	-100.00%	-100.00%	-100.00%
Prompt: few_shot_system			0.4348	0.2083	0.2817	—	0.2708	0.8200	0.3826	0.8000	—	—	0	No	+54.95%	-1.18%	+85.73%
PEFT baselines																	
LoRA (Rank-16) (Hu et al., 2022)			0.5600	0.5833	0.5714	—	0.4583	0.6500	0.2240	0.6300	—	~19MB	Yes	+214.30%	+27.27%	+214.33%	
LoRA (Rank-8) (Hu et al., 2022)			0.4800	0.4500	0.4643	—	0.5200	0.5800	0.1920	0.5600	—	~10MB	Yes	+155.39%	+9.09%	+256.65%	
Prefix-Tuning (Li & Liang, 2021)			0.6174	0.2041	0.3029	—	0.1074	0.8111	0.4405	0.8425	—	~15MB	Yes	+48.76%	+4.63%	-4.58%	
BitFit (Zaken et al., 2022)			0.5873	0.1702	0.2564	—	0.1343	0.7432	0.4323	0.8146	—	~8MB	Yes	+58.98%	+8.49%	-8.93%	
Q-LoRA (Dettmers et al., 2023)			0.7328	0.3154	0.4696	—	0.1193	0.8432	0.4898	0.8922	—	~18MB	Yes	+79.86%	+23.35%	-14.21%	
Vector injection																	
Baseline (zero_shot_system)			0.4400	0.1146	0.1818	0.4844	0.1458	1.0000	0.4000	0.9900	—	0	No	—	—	—	
0.5 ASA (Ours)	steer		0.4615	0.1250	0.1967	0.4896	0.1458	0.9700	0.4231	0.9600	—	~20KB	No	+8.20%	+4.89%	+0.00%	
1.0 ASA (Ours)	steer		0.5937	0.1979	0.2969	0.5312	0.1354	0.9400	0.5625	0.9300	—	~20KB	No	+63.31%	+34.93%	-7.13%	
2.0 ASA (Ours)	steer		0.7805	0.3333	0.4672	0.6198	0.0937	0.8900	0.7073	0.8800	—	~20KB	No	+156.99%	+77.39%	-35.73%	
3.0 ASA (Ours)	steer		0.7778	0.3646	0.4965	0.6302	0.1042	0.8600	0.6667	0.8500	—	~20KB	No	+173.10%	+76.77%	-28.53%	
4.0 ASA (Ours)	steer		0.8718	0.3542	0.5037	0.6510	0.0521	0.8800	0.6923	0.8700	—	~20KB	No	+177.06%	+98.14%	-64.27%	

closing the representation–behavior gap. PEFT baselines such as LoRA can attain strong triggering metrics by updating model weights, but incur non-trivial training/storage overhead and often amplify false triggers; lighter PEFT variants typically preserve post-trigger validity but struggle to recover recall, while quantized variants remain training-dependent. ASA instead offers a *training-free* operating knob with low overhead, achieving competitive triggering behavior while maintaining executability, suggesting its primary effect is targeted control of tool-mode entry rather than improving format compliance alone.

Scaling behavior. Across model scales, the optimal intervention depth shifts with capacity (e.g., L18 → L21), consistent with layer-depth drift under scaling. More importantly, ASA transfers when the base model already possesses tool-calling capability and thus has a latent circuit to amplify; it cannot “create” tool-use behavior from scratch. See Appendix E (Table 14) for the full scaling summary.

4.3. Ablation Study

We ablate ASA at $\alpha = 4.0$ to confirm Table 6 gains are from structured control (not incidental perturbations). **ASA (full)** gives the best balance. Removing the probe-guided gate (No gate) makes injection unconditional and blows up false triggers (FPR = 0.5000), showing the gate is the key safety valve on Non-Tool inputs. A norm-matched Random direction does not help, ruling out a pure “perturbation energy” effect. Composition matters: Global only is strong but less selective, while Domain only is often insufficient to reliably enter tool mode. Mismatch hurts schema consis-

Table 6. Ablation study on test set (Qwen2.5-1.5B, Layer 18, $\alpha = 4.0$). **Oracle Router** uses the ground-truth domain label for domain-vector selection (ideal router with 100% domain accuracy).

Mode	Prec.	Rec.	FPR	Tool acc.
Baseline	0.4400	0.1146	0.1458	0.9600
ASA (full)	0.8718	0.3542	0.0521	0.7436
Oracle Router	0.9714	0.3542	0.0104	0.8000
Global only	0.8261	0.3958	0.0833	0.6957
Domain only	0.3636	0.1250	0.2188	0.7576
No gate	0.4217	0.3646	0.5000	0.7229
Random	0.5556	0.1042	0.0833	0.9444
Mismatch	0.7885	0.4271	0.1146	0.6346

tency, reflected by lower tool-name accuracy. Oracle Router (ground-truth domains) further reduces FPR to 0.0104, indicating routing headroom. **We also report the same ablation pattern on LLAMA in Appendix F**, again highlighting the necessity of gating. LoRA adapters are trained via standard supervised fine-tuning on the same CAL split; full training and generation details are in Appendix C.4.

5. Conclusion

ASA provides a training-free, inference-time control layer for tool-calling domain adaptation, bridging the representation–behavior gap where tool intent is decodable but fails to trigger under strict interfaces. On MTU-Bench, single-shot routed steering with probe-guided gating boosts strict tool-use F1 (higher recall, lower FPR) while preserving output validity.

Impact Statement

This paper presents work on activation steering for tool-calling domain adaptation. The goal is to advance machine learning by improving controllability of large language model agents. Our approach enables reliable tool-calling across domains without parameter updates, potentially reducing deployment costs and improving AI safety through better behavioral control. However, the ability to bidirectionally control tool invocation raises dual use concerns, as adversarial actors might exploit similar mechanisms to suppress safety critical tool calls or evade monitoring systems. We urge researchers to investigate safeguards against unauthorized activation steering. Societal consequences include more robust AI assistants but also potential misuse of steering techniques for deceptive behavior.

References

Bartoszcz, L., Munshi, S., Sukidi, B., Yen, J., Yang, Z., Williams-King, D., Le, L., Asuzu, K., and Maple, C. Representation engineering for large-language models: Survey and research challenges. *arXiv preprint arXiv:2502.17601*, 2025.

Dang, H., Liu, T., Wu, Z., Yang, J., Jiang, H., Yang, T., Chen, P., Wang, Z., Wang, H., Li, H., et al. Improving large language models function calling and interpretability via guided-structured templates. In *Proceedings of the 2025 Conference on Empirical Methods in Natural Language Processing*, pp. 24437–24453, 2025.

Dettmers, T., Pagnoni, A., Holtzman, A., and Zettlemoyer, L. Qlora: Efficient finetuning of quantized llms. *arXiv preprint arXiv:2305.14314*, 2023. doi: 10.48550/arXiv.2305.14314.

Hu, E. J., Shen, Y., Wallis, P., Allen-Zhu, Z., Li, Y., Wang, S., Wang, L., Chen, W., et al. Lora: Low-rank adaptation of large language models. *ICLR*, 1 (2):3, 2022.

Johnson, R. T., Pain, M. D., and West, J. D. Natural language tools: A natural language approach to tool calling in large language agents. *arXiv preprint arXiv:2510.14453*, 2025.

Kwiatkowski, T., Palomaki, J., Redfield, O., Collins, M., Parikh, A., Alberti, C., Epstein, D., Polosukhin, I., Devlin, J., Lee, K., et al. Natural questions: a benchmark for question answering research. *Transactions of the Association for Computational Linguistics*, 7:453–466, 2019.

Lee, B. W., Padhi, I., Ramamurthy, K. N., Miehling, E., Dognin, P., Nagireddy, M., and Dhurandhar, A. Programming refusal with conditional activation steering. *arXiv preprint arXiv:2409.05907*, 2024.

Li, X. L. and Liang, P. Prefix-tuning: Optimizing continuous prompts for generation. *arXiv preprint arXiv:2101.00190*, 2021.

Lu, W., Luu, R. K., and Buehler, M. J. Fine-tuning large language models for domain adaptation: Exploration of training strategies, scaling, model merging and synergistic capabilities. *npj Computational Materials*, 11(1):84, 2025.

Patil, S. G., Zhang, T., Wang, X., and Gonzalez, J. E. Gorilla: Large language model connected with massive apis. *Advances in Neural Information Processing Systems*, 37:126544–126565, 2024.

Prottasha, N. J., Mahmud, A., Sobuj, M. S. I., Bhat, P., Kowsler, M., Yousefi, N., and Garibay, O. O. Parameter-efficient fine-tuning of large language models using semantic knowledge tuning. *Scientific Reports*, 14(1):30667, 2024.

Prottasha, N. J., Chowdhury, U. R., Mohanto, S., Nuzhat, T., Sami, A. A., Ali, M. S., Sobuj, M. S. I., Raman, H., Kowsler, M., and Garibay, O. O. Peft a2z: Parameter-efficient fine-tuning survey for large language and vision models. *arXiv preprint arXiv:2504.14117*, 2025.

Qin, Y., Liang, S., Ye, Y., Zhu, K., Yan, L., Lu, Y., Lin, Y., Cong, X., Tang, X., Qian, B., et al. Toollm: Facilitating large language models to master 16000+ real-world apis. *arXiv preprint arXiv:2307.16789*, 2023.

Rahn, N., D’Oro, P., and Bellemare, M. G. Controlling large language model agents with entropic activation steering. *arXiv preprint arXiv:2406.00244*, 2024.

Schick, T., Dwivedi-Yu, J., Dessì, R., Raileanu, R., Lomeli, M., Hambro, E., Zettlemoyer, L., Cancedda, N., and Scialom, T. Toolformer: Language models can teach themselves to use tools. *Advances in Neural Information Processing Systems*, 36:68539–68551, 2023.

Shinn, N., Cassano, F., Gopinath, A., Narasimhan, K., and Yao, S. Reflexion: language agents with verbal reinforcement learning. In *Advances in Neural Information Processing Systems 36 (NeurIPS 2023)*, 2023.

Stanford, C. Alpaca: a strong, replicable instruction-following model, 2023.

Tang, Q., Deng, Z., Lin, H., Han, X., Liang, Q., Cao, B., and Sun, L. Toolalpaca: Generalized tool learning for language models with 3000 simulated cases. *arXiv preprint arXiv:2306.05301*, 2023.

Turner, A. M., Thiergart, L., Leech, G., Udell, D., Mini, U., and MacDiarmid, M. Activation addition: Steering language models without optimization. 2024.

Wang, G., Xie, Y., Jiang, Y., Mandlekar, A., Xiao, C., Zhu, Y., Fan, L., and Anandkumar, A. Voyager: An open-ended embodied agent with large language models, 2023. 2023.

Wehner, J., Abdnabi, S., Tan, D., Krueger, D., and Fritz, M. Taxonomy, opportunities, and challenges of representation engineering for large language models. *arXiv preprint arXiv:2502.19649*, 2025.

Wu, Z., Arora, A., Wang, Z., Geiger, A., Jurafsky, D., Manning, C. D., and Potts, C. Reft: Representation finetuning for language models. In *Advances in Neural Information Processing Systems 38 (NeurIPS 2024)*, 2024.

Xi, Z., Chen, W., Guo, X., He, W., Ding, Y., Hong, B., Zhang, M., Wang, J., Jin, S., Zhou, E., et al. The rise and potential of large language model based agents: A survey. *Science China Information Sciences*, 68(2):121101, 2025.

Yao, S., Zhao, J., Yu, D., Du, N., Shafran, I., Narasimhan, K. R., and Cao, Y. React: Synergizing reasoning and acting in language models. In *The eleventh international conference on learning representations*, 2022.

Zaken, E. B., Goldberg, Y., and Ravfogel, S. Bitfit: Simple parameter-efficient fine-tuning for transformer-based masked language-models. In *Proceedings of the 60th Annual Meeting of the Association for Computational Linguistics (Volume 2: Short Papers)*, pp. 1–9, 2022.

Zou, A., Phan, L., Chen, S., Campbell, J., Guo, P., Ren, R., Pan, A., Yin, X., Mazeika, M., Domrowski, A.-K., et al. Representation engineering: A top-down approach to ai transparency. *arXiv preprint arXiv:2310.01405*, 2023.

A. Appendix Overview

This appendix complements the main paper with four components. Appendix B explains why intent may be strongly decodable in representation space yet fail to reliably manifest as tool-entry behavior under strict interface constraints. Appendix C specifies datasets, splits, models, decoding, interventions, and metric definitions for faithful replication. Appendix D defines deterministic trigger and validation rules so that the behavioral event $T(x)$ is auditable. Appendix E provides additional results referenced but not expanded in the main text, including cross-model probe decodability, logit-lens causality tables, cross-domain interference matrices, prompt baselines, scaling summaries, and efficiency comparisons.

B. Theoretical Analysis: From Representation to Behavior

B.1. Problem setup and the representation–behavior gap

We study tool calling as an *auditable discrete event* under strict interface constraints. Given an instruction x , the agent produces a string output. A deterministic parser maps the output to a binary event $T(x) \in \{0, 1\}$ that indicates whether tool mode is entered. Importantly, the parser defines a *hard boundary* (e.g., the appearance of `<functioncall>` and a valid payload), so small changes in decoding can flip $T(x)$ discontinuously.

Many LLMs encode tool intent in hidden states: a linear probe on a mid-layer residual stream can separate Tool-Necessary vs Non-Tool with near-perfect AUC (see Appendix E, Table 10). However, a high-AUC intent signal does *not* imply reliable tool-entry behavior, because behavior requires the model to emit a very specific string pattern and schema-compliant JSON under decoding constraints.

B.2. Why strong intent decodability may not translate into tool entry

We highlight three failure mechanisms.

(i) **Discrete parser boundary and early-token competition.** Tool entry often depends on *very early* generation decisions that determine whether the model commits to `<functioncall>`. Even if later-layer representations encode intent, the output may remain in natural language if the early-token logit competition is not sufficiently biased. This motivates *mid-layer causal control* that affects the early distribution over trigger tokens, rather than post-hoc formatting.

(ii) **Interface constraints amplify small formatting errors.** A model can be “toolish” but still fail strict validators: invalid JSON, wrong tool name (schema mismatch), or missing/empty arguments are all treated as failures in deployment. Therefore, any method must improve not only trigger rate but also *post-trigger validity*.

(iii) **Prompt/schema fragility under protocol evolution.** Prompt constraints are implemented at the input level; they can be brittle under distribution shifts, context budget changes, and evolving tool schemas. Demonstrations may increase recall but often increase false triggering on Non-Tool inputs, yielding a poor precision–FPR trade-off (Appendix E, Table 13).

B.3. Implication for method design

The analysis motivates the design of a representation-level controller that is *selective* to avoid spurious triggers through probe-guided gating and *domain-structured* to reduce cross-domain interference (see Appendix E, Table 12). The need for selectivity is informed by findings on trigger token competition (Appendix E, Table 11).

C. Experimental Protocol for Reproducibility

C.1. Datasets and splits

We evaluate tool-mode triggering on the REST test set under a strict parser. We compute intervention directions using a calibration set (CAL) that is disjoint from test. For the MoV vector construction, we use the MOV dataset (320 samples) to estimate mean differences between Tool-Necessary and Non-Tool hidden states.

Table 7. ASA configuration and evaluation protocol.

Item	Setting
Training paradigm	Training-free (statistics only)
Vector construction	MOV (320 samples), $\mu_{\text{pos}} - \mu_{\text{neg}}$
Stored parameters	~ 20 KB (steering vectors + probe weights)
Inference overhead	Single vector addition
Compute resource	Single RTX 4090 (< 24GB VRAM)
Prompt template	<i>GLOBAL_SYSTEM_PROMPT</i>
Prompt structure	Strict System/User/Assistant alignment
Test isolation	Test set excluded from all statistics/training
Parser	Deterministic <i>parse_functioncall</i>
Parsing logic	<i><functioncall></i> tag + JSON / <i>ast.literal_eval</i> fallback
Decoding	Greedy (<i>do_sample=False</i>)
Max new tokens	128
Padding side	Left
Random seed	42 (others within $\pm 3\%$)

Table 8. Deterministic trigger and validation rules used in this paper.

Component	Rule
Tool-mode entry	Trigger iff <i><functioncall></i> appears anywhere in the output
Syntactic validity	Payload inside tags is JSON-parseable (AST fallback allowed)
Schema consistency	<i>name</i> must belong to the domain-specific whitelist
Argument integrity	<i>arguments</i> exists, non-empty, and format-compliant

C.2. Models and decoding

We primarily use Qwen2.5-1.5B-Instruct; we additionally report generalization to Qwen2.5-8B-Instruct and (optionally) a LLAMA-family backbone. Decoding uses greedy generation (*do_sample=False*) to minimize variance in $T(x)$ and make parser outcomes deterministic.

C.3. Intervention definition

Let $h_\ell(x)$ denote the residual-stream representation at a selected depth ℓ (selected by a probe sweep; Figure 3). ASA injects an intent-aligned direction v scaled by α , optionally composed from a global component and a domain expert component. A probe-guided gate determines whether to apply $+v$, apply $-v$ (suppress), or do nothing.

C.4. Metrics

We report trigger-level Precision/Recall/F1/FPR, and post-trigger validity (format/tool-name/args accuracy) under strict validators. Success metrics summarize executability after parsing and schema checks.

This table pins down the methods operational definition, preventing hidden degrees of freedom. Two protocol elements are particularly load-bearing. First, test isolation ensures directions are computed only from CAL/MOV, avoiding optimistic bias from leaking evaluation patterns into steering statistics. Second, deterministic parsing plus greedy decoding makes $T(x)$ stable: improvements cannot be explained by sampling variance or ambiguous scoring. Together, these constraints ensure reported gains correspond to genuine improvements in controllable tool entry and executability under a deployment-like interface.

D. Deterministic Parsing and Validation Rules

We define a strict, deterministic evaluator so that tool calling is auditable. Tool-mode entry is triggered iff *<functioncall>* appears anywhere in the output. After triggering, we validate payload parseability and schema compliance.

Table 9. Intervention sites and limitations relevant to behavior control under strict tool-mode parsing.

Method	Intervention site	Form	Key limitation
Prompt / schema	Input X	$\text{do}(X := X')$	Fragile; may suppress tools via over-constraint
Hidden injection	Mid-layer H_{ℓ^*}	$H_{\ell^*} := H_{\ell^*} + \Delta h$	Can raise recall but often raises FPR without gating
ASA (MoV + gate)	Mid-layer H_{ℓ^*}	Conditional $\Delta h(x)$	Depends on intent evidence / routing accuracy
PEFT (LoRA/SFT)	Parameters θ	$\theta := \theta + \Delta\theta$	Costly retraining; maintenance under churn

Table 10. Cross-model probe AUC at a fixed mid layer (Layer 18) (tool intent vs Non-Tool).

Model	Layer	AUC	p-value
Qwen2.5-0.5B-Instruct	L18	0.9994	< 0.001
Qwen2.5-1.5B-Instruct	L18	0.9996	< 0.001
Qwen2.5-8B-Instruct	L18	0.9989	< 0.001

 Table 11. Logit-Lens intervention on Qwen2.5-1.5B at Layer 18 (target token: $\langle\text{functioncall}\rangle$). Reported p-values compare $+v$ vs random.

α	Mode	ΔLogit (mean)	ΔProb (mean)	p-value
0.25	Plus ($+v$)	+0.2077	+1.38%	2.51×10^{-36}
0.25	Minus ($-v$)	-0.2230	-1.41%	—
0.25	Random	-0.0037	+0.11%	—
1.0	Plus ($+v$)	+0.8359	+5.47%	7.10×10^{-43}
1.0	Minus ($-v$)	-0.9414	-5.46%	—
1.0	Random	-0.0459	-0.22%	—

These rules separate two post-trigger failure modes: wrong tool selection (schema mismatch) and non-executable calls (e.g., missing, empty, or invalid arguments). This decomposition is essential for interpreting recall/FPR trade-offs: while a method may increase trigger frequency, it can simultaneously degrade executability. Under these validators, such degradation is penalized in success precision, even if trigger-level recall improves. Consequently, performance gains under this protocol more closely reflect true deployment value than do relaxed evaluations that accept tool-like natural language.

E. Additional Results and Visualizations

The control locus determines reliability under a discrete parser boundary. Prompt methods intervene at X and are sensitive to phrasing and context budget; they can improve apparent compliance by suppressing tool entry, reducing recall. Unconditional hidden injections move the logit competition but are not selective, often increasing both recall and FPR. ASA adds selectivity via probe-guided gating and domain-structured directions, targeting a better recall-FPR Pareto point. PEFT can be strong but is operationally expensive under API churn, motivating training-free steering.

Near-saturated AUC across scales shows tool intent is linearly accessible in mid-layer representations and is largely scale-invariant. However, high AUC should not be conflated with correct tool calls: behavior requires emitting a strict pattern and schema-valid JSON. This gap motivates using the probe as a *controller* (gating signal) rather than assuming intent decodability implies reliable tool entry.

This is a causal signature: increasing α along $+v$ raises the trigger-token logit/probability, while $-v$ suppresses it, and random directions do not replicate the effect. Therefore v is intent-aligned rather than an “energy injection” artifact. Crucially, this evidence addresses *steerability* but not *selectivity*: without gating, the same causal push can spuriously trigger on Non-Tool inputs, inflating FPR hence the need for probe-guided conditional control.

Table 12. Cross-domain interference matrix (cosine similarity) between domain intent vectors.

Domain	Code	Math	Search	Translation
Code	1.00	0.17	0.37	0.42
Math	0.17	1.00	0.29	0.11
Search	0.37	0.29	1.00	0.03
Translation	0.42	0.11	0.03	1.00

Table 13. Prompt baselines without ASA vector injection.

Variant	Recall (Tool=1)	FPR (Tool=0)	Note
Zero-shot System	0.1146	0.1458	Prompt-only baseline under strict triggering
Few-shot System	0.2083	0.2708	Higher recall but substantially higher false triggers
No System	0.0000	0.0000	Tool mode collapses without system specification

Table 14. Scaling summary across model sizes.

Model	Status	Best config	Observed behavior	Conclusion
0.5B	Fail	–	Recall= 0, FPR= 0	Steering cannot create tool ability if missing
1.5B	Success	L18, $\alpha = 4.0$	Recall↑, FPR↓	Sweet spot: rich semantics and controllability
8B	Success	L21, $\alpha = 3.0$	F1: 0.38 → 0.64	Layer drift; gains after re-tuning

 Table 15. Qwen2.5-8B-Instruct: baseline vs ASA at Layer 21, $\alpha = 3.0$.

Metric	Baseline	ASA (steer)	Δ
Precision	0.5179	0.8500	+0.3321
Recall	0.3021	0.5132	+0.2111
F1	0.3816	0.6400	+0.2584
Accuracy	0.5104	0.7083	+0.1979
FPR	0.2812	0.0625	-0.2187

Diagonal dominance indicates domain directions are distinct, supporting a modular representation of tool intent. Very low similarities (e.g., Search vs Translation) imply near-orthogonal subspaces; a single global direction would inject irrelevant components, likely causing wrong tool names or malformed arguments. Moderate overlaps suggest partial shared structure but not enough to justify a one-size-fits-all direction. This motivates MoV routing: selecting domain experts reduces cross-domain leakage and should improve post-trigger schema validity.

Prompting alone struggles under strict parsing. Few-shot increases recall but also increases FPR, indicating pattern-overgeneralization: the model learns tool-like behavior that leaks into Non-Tool contexts. No-system collapse shows the system message is part of the interface contract; without it, the model fails to enter tool mode at all. This supports the claim that input-level methods are brittle under protocol evolution and distribution shifts.

Scaling separates *capability* from *control*. On 0.5B, the model does not implement tool calling robustly, so steering cannot induce correct tool mode. On 1.5B, mid-layer intervention yields higher recall with lower FPR, indicating intent is both readable and behaviorally pliable. On 8B, the optimal depth shifts deeper, consistent with semantic decision boundaries moving with scale; re-selecting ℓ is essential for transfer.

Both precision and recall improve while FPR drops sharply, indicating selective control rather than indiscriminate triggering. The FPR reduction implies the gate (and/or better depth alignment) suppresses spurious tool-mode

Table 16. Storage/parameter footprint comparison.

Method	Stored artifacts	Footprint
ASA (vectors + router)	$\{v_{\text{global}}, v_{\text{domain}}\}$ + lightweight router	~ 20 KB
LoRA (rank-16, REST train)	LoRA adapters (rank-16)	~ 19 MB

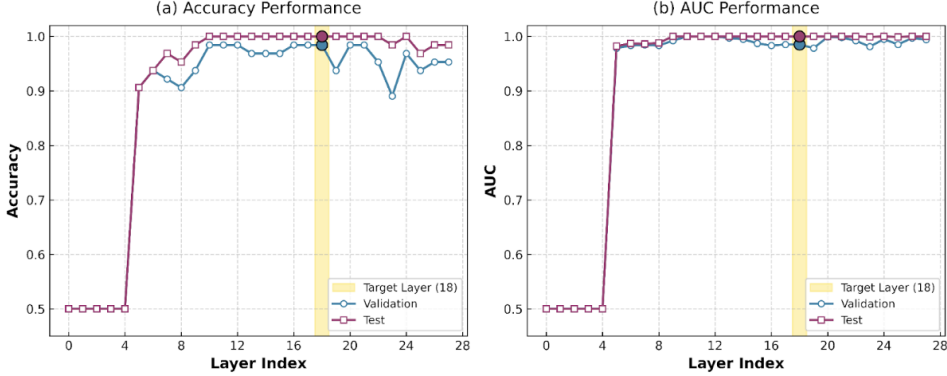


Figure 3. Layer-wise probe sweep used to select the intervention depth.

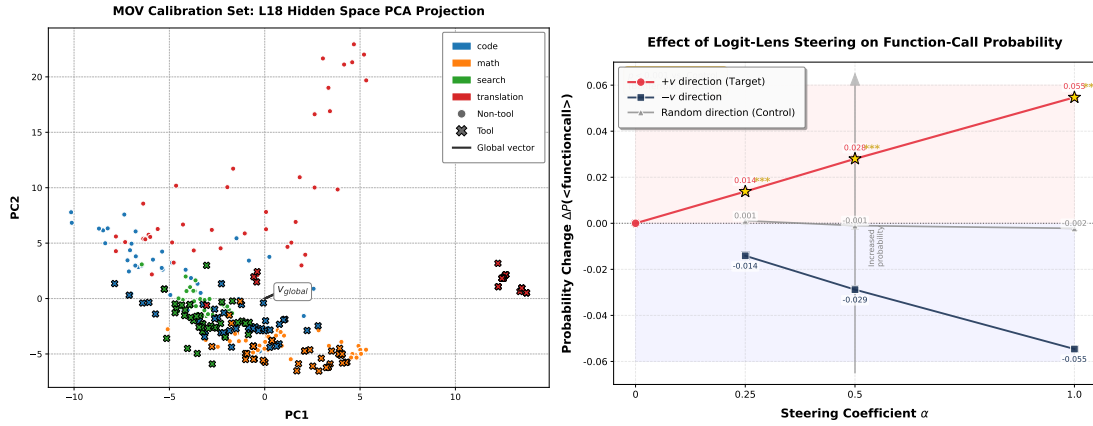


Figure 4. Combined geometry and causal diagnostic at the selected layer.

entry on Non-Tool inputs. Meanwhile recall gains show Tool-Necessary inputs are pushed across the strict trigger boundary. The combined effect yields a strong F1 improvement and validates transfer at scale after depth re-tuning.

The KB-vs-MB footprint gap is decisive under API/tool churn. ASA stores only a few directions and a lightweight controller, making versioning and redeployment cheap. LoRA introduces persistent adapter weights and typically requires retraining/revalidation when schemas change, increasing maintenance cost. Thus, ASA targets a deployment regime where meaningful behavioral gains are achieved with minimal storage and no gradient updates.

Discussion of Figure 3. Figure 3 defines the depth selection criterion: we choose ℓ where validation separability peaks (or forms a stable plateau), indicating a well-formed intent boundary. Intervening too early can be “pre-semantic” and unstable; intervening too late can reduce controllability because downstream transformations are constrained by decoding dynamics. Fixing ℓ based on validation prevents test overfitting and ensures steering results reflect a principled depth choice rather than post-hoc tuning.

Discussion of Figure 4. In Figure 4, the geometry component supports a structured representation where Tool

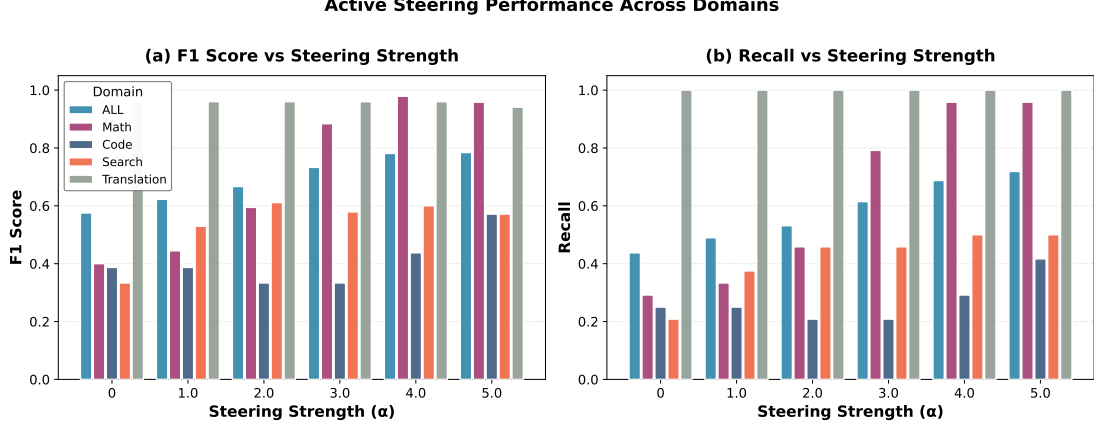


Figure 5. Active steering performance on REST: domain-wise trends versus intervention strength α .

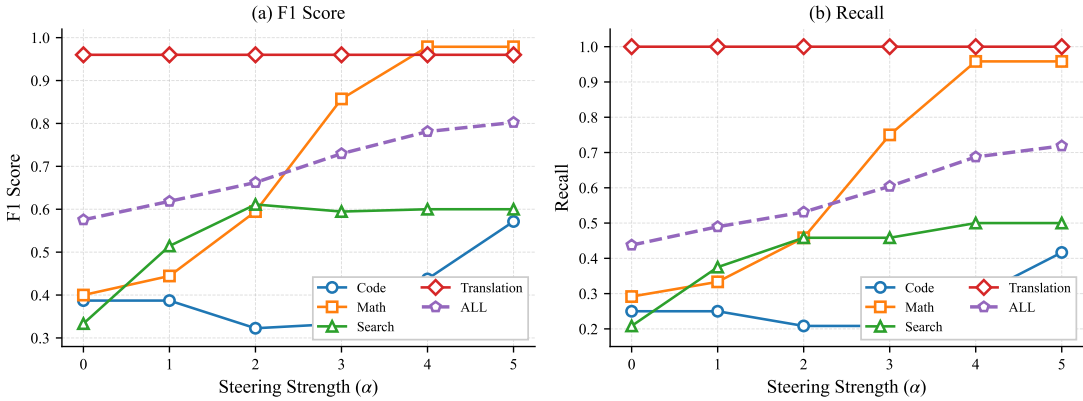


Figure 6. REST: F1/Recall curves across domains under different steering strengths α .

vs Non-Tool (and often domains) occupy separable regions; this motivates domain-structured experts rather than a single global direction. The causal component shows direction-specific control (aligned vs anti-aligned effects) and rejects the “random energy” explanation. Together, Figure 4 justifies two key design choices: intent-aligned vectors exist and are causally meaningful, but selectivity is still required to avoid spurious triggers.

Discussion of Figure 5. Figure 5 visualizes the operating-point movement induced by α . Low α is insufficient to consistently reorder early decoding decisions, limiting recall improvements. Moderate α increases the chance that Tool-Necessary inputs cross the strict trigger boundary, improving recall/F1. Overly large α can dominate downstream computation, increasing spurious triggers or schema instability; this is exactly where probe-guided gating is necessary to preserve precision and control FPR.

Discussion of Figure 6. The curves in Figure 6 reveal domain-dependent sensitivity to α . Some domains saturate recall quickly (strong intrinsic tool prior), while others require larger α but risk higher FPR or post-trigger errors. This heterogeneity in Figure 6 argues against a single global setting and supports routing + gating: the intervention should be conditioned on domain and intent confidence to reach each domains best operating region.

Discussion of Figure 7. Reporting the best per-domain operating point in Figure 7 prevents aggregate metrics from hiding domain regressions. The selected α also indicates “control difficulty”: domains requiring larger α likely have weaker natural trigger evidence under strict parsing. This supports the need for conditional control: rather than brute-force amplification, gating can preserve precision while still enabling recall gains where needed.

Discussion of Figure 8. The heatmap in Figure 8 makes the global trade-off explicit: recall often rises with α

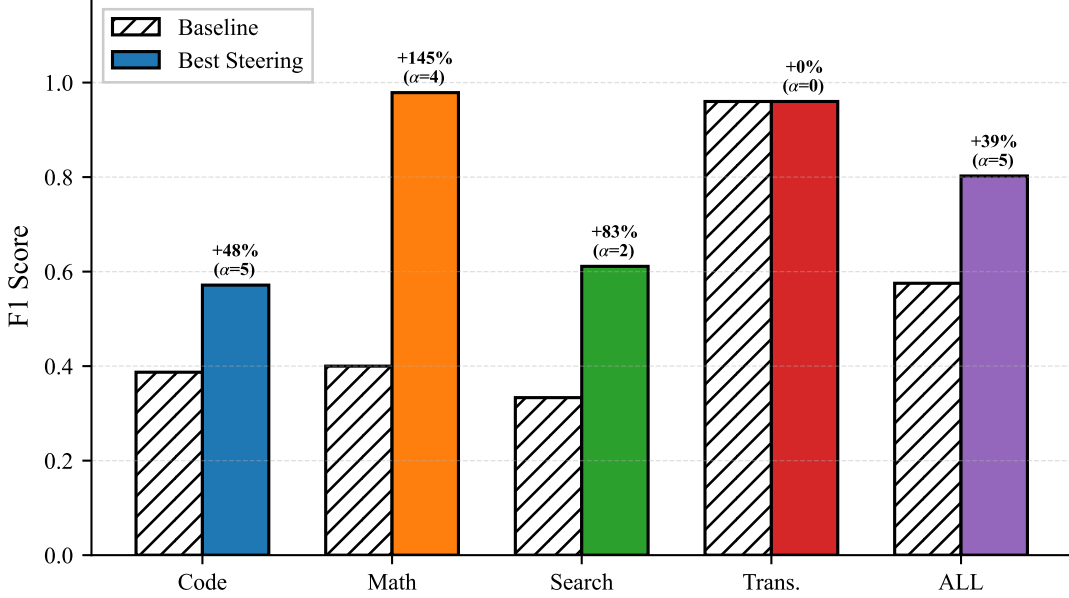


Figure 7. REST: F1 improvement at the best operating point per domain (annotated with the selected α).

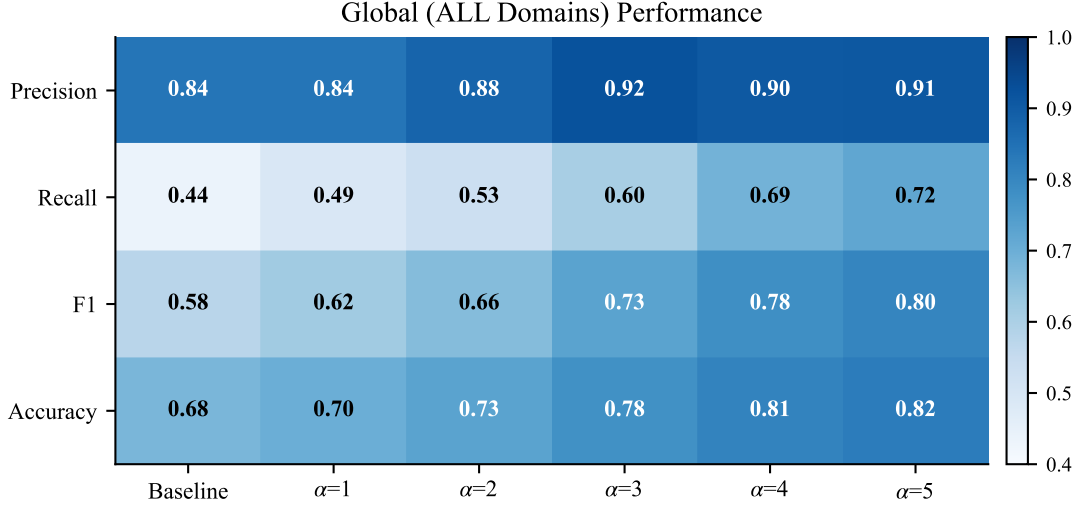


Figure 8. REST (ALL domains): global metrics as a function of α .

up to a point, but precision can degrade if FPR increases. Therefore, “bigger α ” is not optimal; the best region is where recall gains do not trigger a disproportionate increase in spurious tool-mode entries. This emphasizes why we report both recall and FPR and tune α on validation rather than maximizing trigger frequency.

F. Ablation Studies

Full ASA shifts the operating point substantially: precision and recall both rise while FPR drops, yielding a large F1 gain evidence of selective control rather than increased trigger frequency alone. The **no_gate** ablation isolates the gates safety role: recall rises but FPR explodes, a characteristic failure mode of unconditional amplification. The **random** direction control does not improve F1, ruling out a generic perturbation-energy explanation. Composition matters: **global_only** boosts recall but retains higher FPR; **domain_only** underperforms and increases FPR, consistent with insufficient shared intent evidence. Finally, **no_router** achieves extremely low

Table 17. Ablation study on the ALL domain. Precision/Recall/F1/Accuracy/FPR are computed for tool-mode triggering under the strict protocol.

Ablation Mode	Strategy	Precision	Recall	F1-Score	Accuracy	FPR
full	baseline	0.440	0.115	0.182	0.484	0.146
full	steer	0.872	0.354	0.504	0.651	0.052
no_router	baseline	0.440	0.115	0.182	0.484	0.146
no_router	steer	0.971	0.354	0.519	0.672	0.010
global_only	baseline	0.440	0.115	0.182	0.484	0.146
global_only	steer	0.826	0.396	0.535	0.656	0.083
domain_only	baseline	0.440	0.115	0.182	0.484	0.146
domain_only	steer	0.364	0.125	0.186	0.453	0.219
no_gate	baseline	0.440	0.115	0.182	0.484	0.146
no_gate	steer	0.422	0.365	0.391	0.432	0.500
random	baseline	0.440	0.115	0.182	0.484	0.146
random	steer	0.556	0.104	0.175	0.510	0.083
mismatch	baseline	0.440	0.115	0.182	0.484	0.146
mismatch	steer	0.788	0.427	0.554	0.656	0.115

Table 18. Post-trigger validity under the steer strategy. Component accuracies are computed conditional on triggering.

Ablation Mode	Call Count	Format Acc	Tool Name Acc	Args Acc	Success Recall	Success Precision
full	39	0.949	0.744	0.949	0.281	0.692
no_router	35	0.943	0.800	0.943	0.281	0.771
global_only	46	0.978	0.696	0.978	0.323	0.674
domain_only	33	0.970	0.758	0.970	0.115	0.333
no_gate	83	0.976	0.723	0.976	0.292	0.337
random	18	1.000	0.944	1.000	0.094	0.500
mismatch	52	0.962	0.635	0.962	0.333	0.615

FPR while preserving recall, implying routing errors are a bottleneck and improving routing is a high-leverage path forward.

Most variants maintain high format/args accuracy, suggesting the intervention primarily affects *whether* the model enters tool mode rather than causing systematic JSON collapse. Tool-name accuracy is the most sensitive dimension: routing/direction mismatch increases schema errors. **no_gate** triggers far more often but has very low success precision, demonstrating the deployment failure mode of over-triggering. **no_router** improves success precision, reinforcing that routing errors translate directly into wrong tool names/arguments and represent a key bottleneck for further improvements.

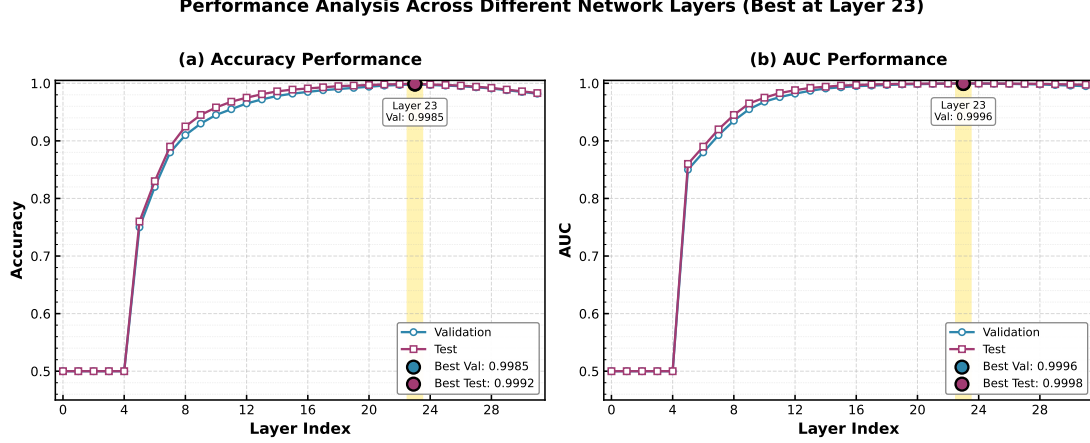


Figure 9. LLAMA: layer-wise probe decodability sweep over 32 layers.

A clear peak/plateau indicates tool intent becomes linearly accessible at certain depths, but the optimal layer can differ from Qwen due to architectural/training differences. This figure justifies re-running layer selection per backbone; reusing Qwens ℓ blindly can be suboptimal. Conceptually, it supports the claim that intent decodability is common while the depth at which it is most actionable is model-dependent.

Table 19. Injection instances (baseline text vs injected function-call text) with strict validity scores.

Index	Domain	Baseline (excerpt)	Injected text (exact)	Fmt	Tool	Args	Task
1	math	(baseline...) “To calculate ...”	<code><functioncall>{"name": "calculator", "arguments": {"expression": "3 1.0 + 4 + 3" }}</functioncall></im_end ></code>				
7	search	<code><functioncall>...</code>	<code><functioncall>{"name": "web_search", "arguments": {"query": "magick sustainable living 5" }}</functioncall></code> <code><functioncall>{"name": "web_search", "arguments": {"query": "images recycling 5" }}</functioncall></im_end ></code>				
18	math	(baseline...) “Discounted Price...”	<code><functioncall>{"name": "calculator", "arguments": {"expression": "\$200 * (1 - 0.2)" }}</functioncall></im_end ></code>				
23	math	(baseline...) “Discounted Price...”	<code><functioncall>{"name": "calculator", "arguments": {"expression": "\$200 * (1 - 0.2)" }}</functioncall></im_end ></code>				
24	code	(baseline...) “def calculate...”	<code><functioncall>{"name": "python_interpreter", "arguments": {"code": "import numpy as np\\nnp.min([10, 20, 30]) - np.max([10, 20, 30])" }}</functioncall></im_end ></code>				

Analysis of Table 19. This table clarifies what “strict post-trigger validity” means in practice. Case 7 is especially diagnostic: the baseline already looks tool-like but lacks consistent closing tags, which can fail strict validators; the injected version repairs the delimiter structure while preserving semantic intent, yielding perfect format/tool/args scores. Across cases, the injected outputs are fully schema-formed `<functioncall>` blocks, which is necessary for deployment executability under Appendix D.

G. Injection Examples (Baseline vs Injected)

Table 20. Raw injection JSON records (verbatim) used for Appendix G.

```
[
  {
    "index": 1,
    "domain": "math",
    "instruction": "Okay, here they are. I took Math with a grade of A...",
    "baseline_text": "To calculate your total GPA...",
    "injected_text": "<functioncall>{\\"name\\": \\"calculator\\", \\"arguments\\": {\\"expression\\": \\"3 + 4 + 3\\\"}}</functioncall><|im_end|>",
    "format_score": 1.0, "tool_name_score": 1.0, "args_score": 1.0, "task_score": 1.0
  },
  {
    "index": 7,
    "domain": "search",
    "instruction": "I need images related to \"sustainable living\"...",
    "baseline_text": "<functioncall>{\\"name\\": \\"web_search\\\"...",
    "injected_text": "<functioncall>{\\"name\\": \\"web_search\\", \\"arguments\\": {\\"query\\": \"images sustainable living 5\\\"}}</functioncall>\n<functioncall>{\\"name\\": \\"web_search\\", \\"arguments\\": {\\"query\\": \"images recycling 5\\\"}}<|im_end|>",
    "format_score": 1.0, "tool_name_score": 1.0, "args_score": 1.0, "task_score": 1.0
  },
  {
    "index": 18,
    "domain": "math",
    "instruction": "I saw a dress that I liked...",
    "baseline_text": "To calculate the discounted price...",
    "injected_text": "<functioncall>{\\"name\\": \\"calculator\\", \\"arguments\\": {\\"expression\\": \\"$200 * (1 - 0.2)\\\"}}</functioncall><|im_end|>",
    "format_score": 1.0, "tool_name_score": 1.0, "args_score": 1.0, "task_score": 1.0
  },
  {
    "index": 24,
    "domain": "code",
    "instruction": "I have an array of numerical entities...",
    "baseline_text": "To calculate the range...",
    "injected_text": "<functioncall>{\\"name\\": \\"python_interpreter\\", \\"arguments\\": {\\"code\\": \\"import numpy as np\\nnp.min([10, 20, 30]) - np.max([10, 20, 30])\\\"}}</functioncall><|im_end|>",
    "format_score": 1.0, "tool_name_score": 1.0, "args_score": 1.0, "task_score": 1.0
  }
]
```

Analysis of Table 20. This verbatim record ensures the injection examples are auditable and reproducible. Notably, the injected texts enforce complete tag closure and schema-complete JSON payloads with *name* and *arguments*. Under the deterministic rules in Table 8, these surface-form constraints are necessary: even semantically correct intentions can fail deployment if the emitted string is not strictly executable.